DRP-1-15
April 1994

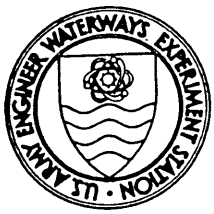

Dredging Research Technical Notes

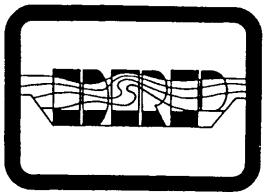

Erosion by Entrainment of Fluidized Cohesive Sediments

Purpose

This technical note describes cohesive sediment erosion by the entrainment process, which can be important to the open-water dispersion of fluidized dredged material. Some specific predictive algorithms are presented.

Background

Entrainment occurs when a turbulent fluid layer incorporates fluid from an adjacent layer into itself. Entrainment is a fluid process that can be important to cohesive sediment dispersion in the following dredging-related situations:

- During the convective descent phase at disposal.
- Just after disposal at the leading edge of a rapid-spreading underflow.
- Following disposal if a residual fluid mud layer is formed.
- After fluidization of disposed sediments by waves or other conditions.
- In navigation channels near agitation or overflow dredging.

Situations in which entrainment occurs can thus be grouped into two categories depending on whether entrainment occurs at horizontal or vertical interfaces. The first two situations above represent the vertical category. All other dredged material cases involve stable, approximately horizontal interfaces. This distinction determines whether density differences control the respective entrainment and whether the entrainment is considered an erosion process.

Entrainment involving horizontal density layers is an important erosion process that can mobilize disposed sediments for transport offsite. Entrainment in cases of vertical interfaces is not inhibited by density differences. The general concept of entrainment can be applied to a number of related

US Army Engineer Waterways Experiment Station
3909 Halls Ferry Road, Vicksburg, MS 39180-6199

geophysical processes and has been used in models such as the Corps' STFATE disposal model and other near-field models.

Erosion by entrainment is controlled by density differences between the layers, particle settling, and viscosity of the suspension as well as flow conditions. Entrainment can occur when cohesive sediments are in a fluid state, sometimes called fluid muds, with relatively low concentrations ranging from about 5 to 300 g/L, depending on sediment properties. At higher concentrations, sediment properties change rapidly and other erosion processes come into play, such as those described in *Dredging Research Technical Notes* DRP-1-07 (Teeter 1992a). At lower concentrations, settling properties of cohesive sediments will not establish a sharp lutocline—a region of high vertical gradient in sediment concentration.

The Dredging Research Program (DRP) Technical Area "Analysis of Dredged Material Placed in Open Water" is testing entrainment process descriptors, and enhancing them as necessary to accurately describe dredged material entrainment. This technical note presents background information on the entrainment process as it applies to dredged sediments and describes intermediate results in algorithm development.

Additional Information

Contact the author, Mr. Allen Teeter, (601) 634-2820, or the manager of the Dredging Research Program (DRP), Mr. E. Clark McNair, (601) 634-2070, for additional information.

Introduction

A fluid mud layer lying at the bottom of a water body can be defined as having three regions in the vertical dimension. Vertical layering above a given dense layer suspension is shown in Figure 1 for high- and low-current cases. The upper region is called the mixed layer and is assumed to be turbulent. The intermediate layer is called the stable layer, lutocline, or interfacial layer; its presence depends on the entrainment process. The intermediate layer may move with the flow and be at least partially turbulent. The lower layer is called the dense layer. It is stationary or slowly moving as a laminar flow. Because of their relatively low settling velocities and cohesive properties, fine-grained sediments can remain in a fluid state and susceptible to entrainment for long periods. Surface waves can fluidize cohesive sediments, as described in *Dredging Research Technical Notes* DRP-1-14 (Teeter 1994).

Net entrainment through the lutocline will depend on conditions in both the mixed layer and the dense layer and thus will generally be time and space dependent. The net entrainment (E) across the fluid mud dense layer interface is the difference between the upward turbulent (F_t) and downward settling (F_s) vertical flux components. Thus,

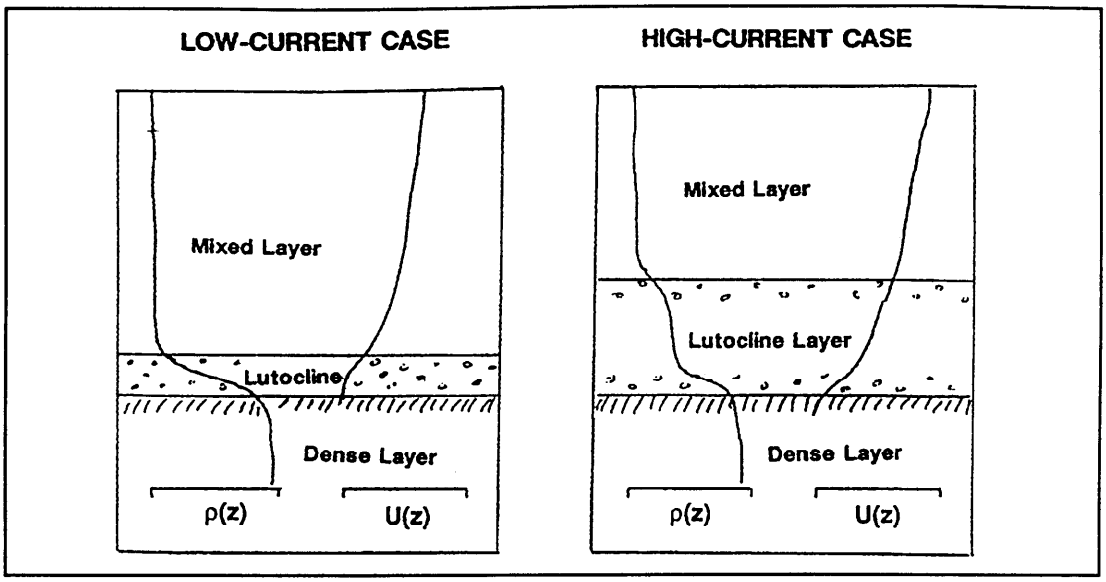

Figure 1. Vertical structure above a fluid mud layer for low- and high-current cases

$$E = F_t - F_s \quad \text{for } F_t > F_s \tag{1}$$

The turbulent component, F_t, is initiated by motions generated by the mixed-layer flow which penetrate the lutocline layer, and is the flux rate at which sediment is mixed upward from the dense layer. (A notation listing is provided as Table 1.)

One of the main controls for the turbulent component, F_t, is the overall density difference between the mixed and dense layers. The relative buoyancy change across the interface is $\Delta b = g(\rho_m - \rho_o)/\rho_o$ for dense fluids and $\Delta b = g(C_m - C_b)(\rho - \rho_l)/\rho_s\rho_o$ for suspensions, where g is the acceleration of gravity. Variables ρ_m, ρ_o, ρ_l, and ρ_s are the densities of the fluid mud, mixed layer, fluid, and solid particles, respectively, and C_m and C_b are the solids concentrations just below and above the interfacial layer. Therefore, for suspensions, the density difference (in kilograms per cubic meter or grams per liter) between the mixed and dense layers is normally about 0.61 times the sediment concentration difference in grams per liter.

A velocity depicting the rate of interfacial displacement, V_t, due to turbulent entrainment is $F_t/(\rho_m - \rho_o)$ for dense fluids. For suspensions, $V_t = F_t/(C_m - C_b)$, where F_t represents the flux of solids. The turbulent velocity, V_t, can be scaled by a characteristic velocity, for example the mean mixed layer velocity, U, to form a nondimensional entrainment. An interface displacement rate due to settling is defined as $Ws_i = (WsC_b)/(C_m - C_b)$ where Ws is the settling rate and WsC_b is the settling flux just above the interface. Then, a nondimensional entrainment for a suspension is $(V_t - Ws_i)/U$, for example.

Table 1
Notation Definitions

Notation	Definition
a	Amplitude of an oscillating grid, m
C_b	Solids content at the bottom of the mixed layer, kg/cu m or g/L
C_m	Solids content at upper edge of the dense layer, kg/cu m g/L
D	Mixed layer depth, m
E	Net entrainment, kg/sq m/sec
F_t	Upward turbulent flux, kg/sq m/sec
F_s	Downward settling flux, kg/sq m/sec
g	Gravity, m/sq sec
h	Interfacial layer thickness, m
$k1, k1$	Viscosity criteria constants
K	Turbulent entrainment constant
Kz	Vertical eddy diffusivity, sq m/sec
Kz_o	Depth-averaged Kz for nonstratified conditions, sq m/sec
Re	Reynolds number for the mixed layer
Ri_g	Gradient Richardson number
Ri_u	Richardson number scaled by U
Ri_*	Richardson number scaled by U_*
U	Mixed layer current speed, m/sec
U_*	Mixed layer shear velocity, m/sec
V_t	Upward entrainment velocity, m/sec
Ws	Settling rate, m/sec
Ws_i	Interfacial displacement rate due to settling, m/sec
z	Vertical coordinate, m
Δb	Buoyancy difference
η_m	Mud viscosity, $Pa \cdot sec$
η_o	Viscosity of mixed layer, $Pa \cdot sec$
ρ_o	Mixed layer density, kg/cu m
ρ_l	Fluid density, kg/cu m
ρ_m	Density of mud, kg/cu m
ρ_s	Particle density, kg/cu m
τ	Shear stress, Pa
ω	Angular frequency, radians/sec

The remainder of this technical note will address entrainment as an erosion process of cohesive sediments. Four mechanisms important to the entrainment of cohesive suspension layers are described in the sections that follow: density stratification, viscosity, settling, and layer thickness. These mechanisms act to control entrainment, while the entrainment process is the net effect of multiple mechanisms.

Density Stratification Effects

Upward turbulent flux of material results from instabilities and recoils at the upper surface of the lutocline and from intermittent turbulence and internal wave motions that reach the dense layer. For horizontal layers, density differences control how much energy goes into mixing in the absence of other mechanisms. The greater the density difference between the layers in relation to the inertial forces, the lower the E. In simple cases, the turbulent entrainment component can be described using an overall Richardson number, Ri, relating buoyancy and inertial forces. The most appropriate scaling for Ri numbers is the mixed layer depth, D, and mean velocity, U, although for mixed layers without mean-shear (such as tanks with oscillating grids), the shear velocity, U_*, is used. Then, for ordinary flowing and purely turbulent mixed layers,

$$Ri_u = \frac{\Delta b\, D}{U^2} \quad \text{and} \quad Ri_* = \frac{\Delta b\, D}{U_*^2} \qquad \text{(2a, b)}$$

Equation 2b applies to experiments where artificially generated turbulence is used, as will be described later.

When settling and viscous effects are absent, fluid mud is entrained in the same manner as a dense fluid. Figure 2 shows entrainment data obtained by Narimousa and Fernando (1987) and Srinivas and Mehta (1989) using similar racetrack-type flumes wherein flows were driven by disk pumps. The Narimousa and Fernando (1987) data are for salt layers, while the Srinivas and Mehta (1989) data are for kaolinite-clay suspension dense layers. Kaolinite is a common commercial clay mineral that is not particularly cohesive and whose settling rate is much lower than most natural cohesive sediments.

In the case of the kaolinite suspension data, the Ws_i is very small; therefore, $(V_t - Ws_i)/U$ is equivalent to V_t/U. The Srinivas and Mehta (1989) suspensions had concentrations of 50 to 133 g/L clay mixed with tap water. The mixed layer mean velocity, U, ranged from 50 to 100 mm/sec, while Ws in the dense layer was probably on the order of 0.002 mm/sec or less. The stable layer thickness, h, with respect to the depth, D, was about the same for both the Srinivas and Mehta (1989) and Narimousa and Fernando (1987) tests.

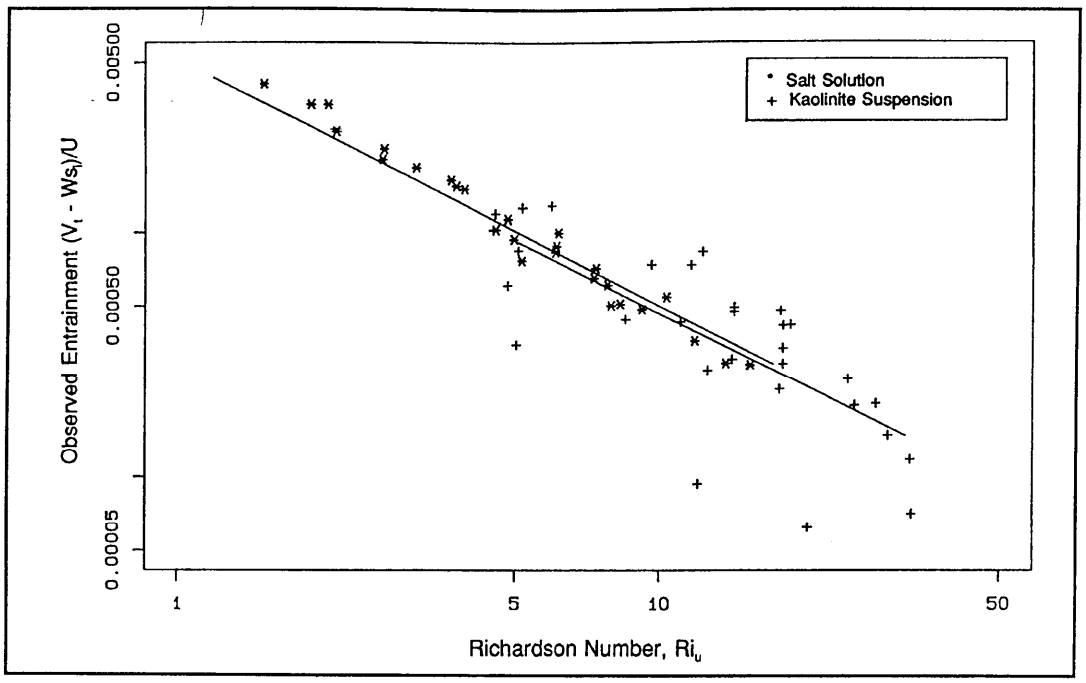

Figure 2. Entrainment for a dense fluid and fluid mud as a function of Ri_u

The line in Figure 2 associated with the Narimousa and Fernando (1987) salt solution data is a -1 power law fit by the original author, and since no settling was associated with the salt data, the observed nondimensional entrainment is equivalent to V_t/U. The line associated with the Srinivas and Mehta (1989) data is a regression fit to the log-transformed total entrainment data, which also shows a -1 power dependence of $(V_t - Ws_i)/U$ on Ri_u.

As shown in Figure 2, $(V_t - Ws_i)/U$ or V_t/U for both data sets had similar functional relationships with Ri_u, at least over most of the Ri_u range. A few of the high-Ri_u kaolinite data points have reduced entrainment values, and it was reported that, at Ri_u of about 25, turbulent entrainment at the interface ceased as the result of suppression of turbulence. Overall, the data in Figure 2 represent conditions of entrainment where suspensions were unaffected by settling or suspension viscosity. The lines for salt and kaolinite density-stratified cases shown in Figure 2 are similar because the entrainment process was controlled primarily by density differences.

In the *Ri* range normally involving fluid muds, various general functional forms have been proposed on theoretical grounds and supported by various data sets, the most widely used being power laws with -3/2 or -1 slopes. Arguments for a particular functional relationship are based on either energy considerations or eddy impingement. Work is performed by the mixed layer as dense material is entrained vertically and the potential

energy of the system is changed. Based on data presented in Figure 2 and by others, it is proposed that

$$F_t = K(C_m - C_b)\, U\, Ri_u^{-1} \text{ for } \rho_m UD/\eta_m > k2 \tag{3}$$

where K is a constant, η_m is the dynamic viscosity of the mud, and the second expression is a viscosity criterion based on a constant $k2$, which is described in the section "Mud Viscosity Effects."

At low Ri values, the lutocline can become largely turbulent, as depicted in the high-current case in Figure 1. Turbulent flux, F_t, is generally time dependent and is a function of vertical turbulent diffusion and vertical concentration gradient values, as described by

$$F_t = Kz(z)\frac{\partial C}{\partial z} \tag{4}$$

where Kz is the vertical eddy diffusivity and the parenthetical z indicates a value at a given point in the vertical. These conditions must normally be calculated numerically using various computer algorithms. For example, the vertical diffusion can be calculated according to Teeter and Pankow (1989) as

$$Kz(z) = f(z)\, Kz_0 [1 + 33\, Ri_g(z)]^{1.5} \tag{5}$$

where $f(z)$ describes the vertical distribution of $Kz(z)$, Kz_0 is a depth-averaged vertical diffusion value for homogeneous conditions, and Ri_g is the local gradient Richardson number given by

$$Ri_g = \frac{-g\partial \rho_o / \partial z}{\rho_o (\partial U/\partial z)^2} \tag{6}$$

Wolanski and others (1988) used a similar method to obtain predictions that were in good agreement with field measurements.

Mud Viscosity Effects

The turbulent component, F_t, can be modified by viscous effects. If the fluid mud layer viscosity exceeds a certain level, interfacial instabilities and turbulent entrainment flux rapidly diminish. Entrainment

suppression has been observed to occur when viscous and inertial forces are comparable at the turbulent scale of the entraining flow (Campbell and Turner 1986). Wide, open channels, for instance, have length scales for vertical turbulence approximately equal to the flow depth, and the velocity scale is equal to the mean flow speed. The mixed layer criterion for entrainment is a Reynolds number for that layer.

$$\mathrm{Re} = \rho_m U D/\eta_o > \eta_m/\eta_o \qquad (7)$$

where U is the average flow speed of the mixed layer, D is the channel depth, and η_o and η_m are the dynamic viscosities of the mixed and dense layers, respectively. Thus, entrainment begins to be suppressed when $\rho_m U D < \eta_m$.

On theoretical grounds, Campbell and Turner (1986) proposed that the viscosity effect can be described by two values (*k1* and *k2*) of the parameter *k*, where $k = \rho_m UD/\eta_m$. Complete suppression of entrainment occurred at k1, and partial suppression occurred between *k1* and *k2*, with a linear transition between. Campbell and Turner (1986) estimated k1 = 7 and k2 = 70. A plot of their data is shown in Figure 3. Based on the present reanalysis of these data, the values *k1* = 5 and *k2* = 85 seem more appropriate.

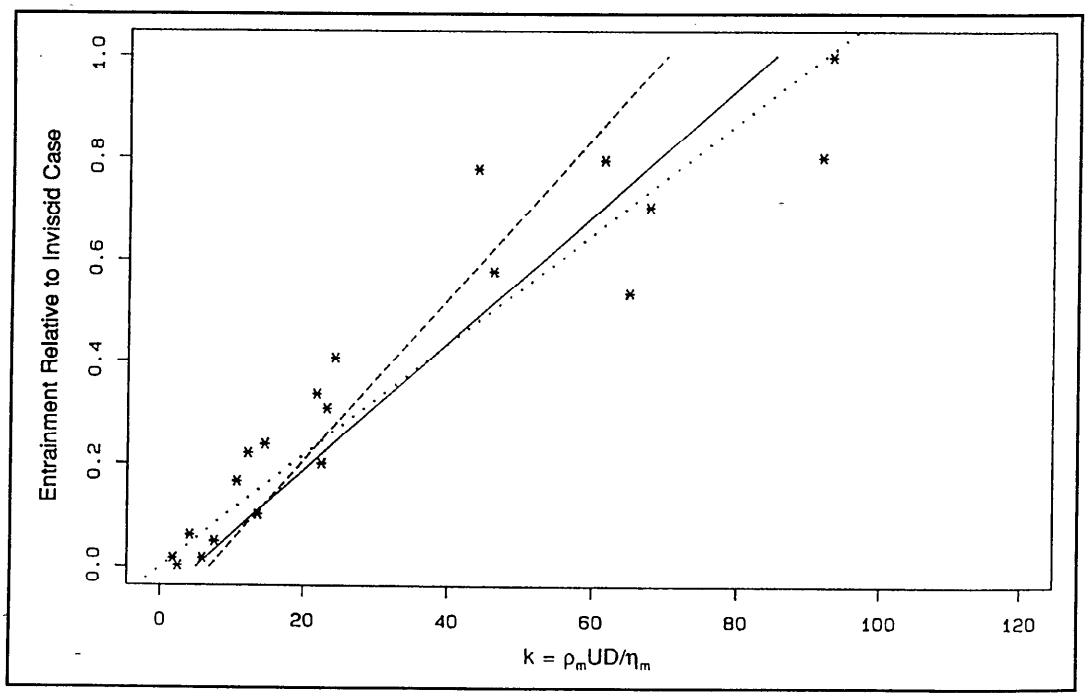

Figure 3. Relative entrainment according to Campbell and Turner (1986) [points]; for their suggested k1 = 7 and k2 = 70 [dashed line]; a regression fit to their data [dotted line]; and for the proposed k1 = 5 and k2 = 85 [solid line]

Viscosity constraints can be placed on F_t for suspensions as follows:

$$F_t = \left[\frac{\rho_m UD - k1\,\eta_m}{(k2-k1)\eta_m}\right] K\,(C_m - C_b)\,URi_u^{-1}, \quad k1 < \rho_m UD/\eta_m < k2 \tag{8}$$

$$F_t = 0, \quad \rho_m UD/\eta_m < k1 \tag{9}$$

The viscosities of fluid mud vary widely with its density, ρ_m, or concentration, C_m. While adequate information exists to propose descriptors for entrainment suppression by viscosity effects in negatively buoyant plumes and dense suspension layers, the most appropriate viscosity characterization has not yet been confirmed. Fluid mud is a shear-thinning material, usually exhibits thixotropy, and can be fluidized by pressure fluctuations. Over narrow ranges of shear rates and shear stresses, the viscosity of a given fluid mud can vary by orders of magnitude (*Dredging Research Technical Notes* DRP-02-04, Teeter 1992). Density-viscosity values have been found to vary widely between sites, with temperature, and as the result of other factors.

Figure 4 shows a plot of observed viscosity versus shear stress for fluid

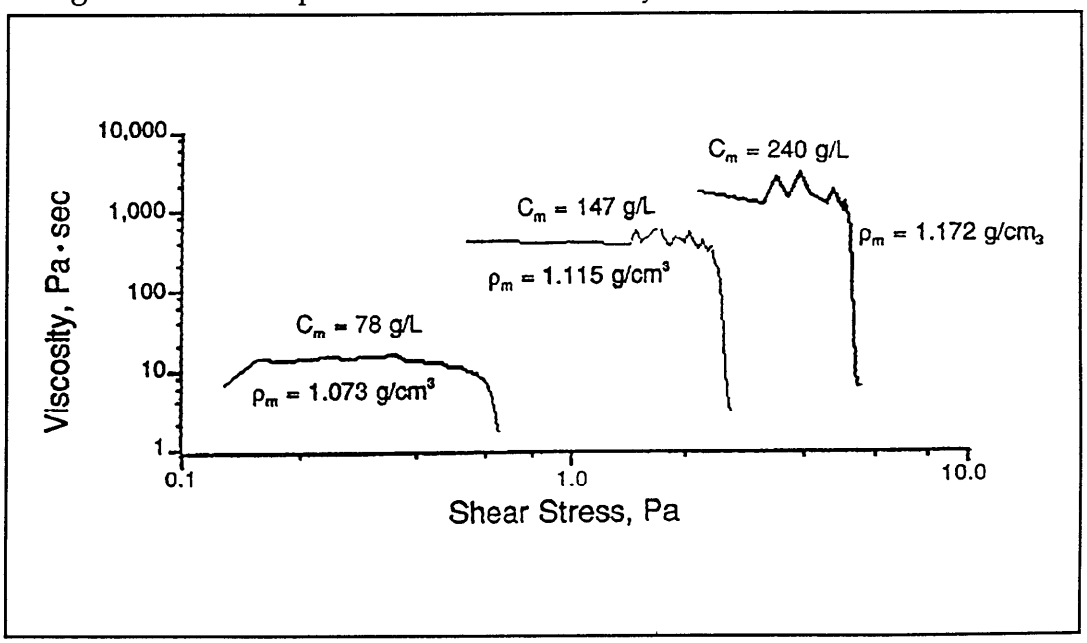

Figure 4. Viscosity of three Sabine River, Texas, sediment samples over a range of shear stresses

mud from the Sabine Entrance Channel, Texas, at three densities. Variations in viscosity for a single material are large, and at some threshold shear stress value, viscosity drops markedly. For the range of shear stresses normally encountered, say less than 1 Pa, Table 2 provides

example data on the relationship between solids content, bulk wet density, and viscosity for a cohesive material.

Table 2
Example Cohesive Material Characteristics

C_m, g/L	ρ_m, kg/cu m	η_m, Pa sec
24	1,040	1
41	1,050	5
81	1,075	10
106	1,090	50
163	1,125	200

Water has a viscosity, η_o, of about 0.001 Pa • sec. Using density versus viscosity data such as these and disposal site information, the nomogram shown in Figure 5 can be used to judge the extent of viscosity effects.

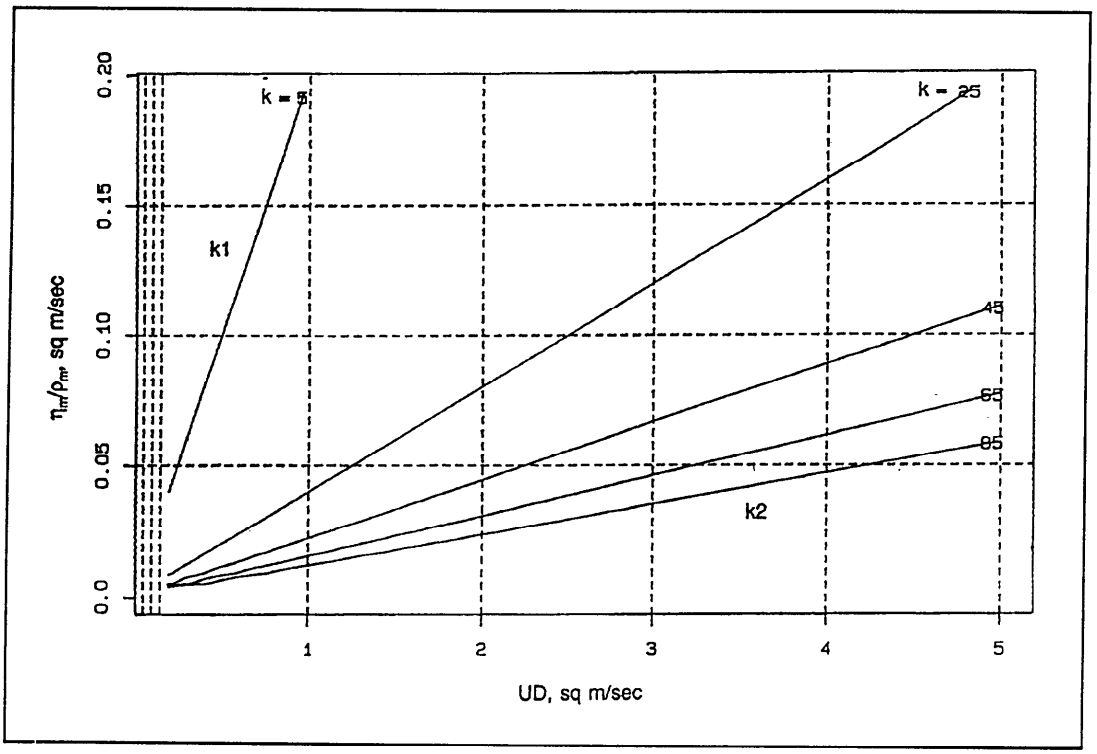

Figure 5. Nomogram showing k-values for complete entrainment suppression (k = 5), entrainment reduction (5 < k < 85), unhindered entrainment (85 < k) as functions of UD and η_m/ρ_m

Entrainment in cases of vertical interfaces is not inhibited by density differences, although at high concentrations, cohesive sediment viscosity may inhibit entrainment in these cases. Sediment characteristics have been

previously shown to affect entrainment coefficients and rates. For instance, negatively buoyant plume entrainment rates were found to decrease rapidly and approach zero as moisture contents approached the liquid limits for the material (Bowers and Goldenblatt 1978). Those previous results can now be interpreted in light of newer, more general experimental and theoretical results on liquids of different viscosity.

Particle Settling Effects

Fluid mud settling counteracts upward entrainment as described earlier. The settling flux, F_s, depends upon properties of the sediment material, concentration of suspended sediment, and other conditions in the mixed or lutocline layer. The settling flux can be calculated for any vertical location as

$$F_s = Ws\,(z)\;\; C_b\,(z) \tag{10}$$

If conditions are steady, F_s can be evaluated at the bottom of the mixed layer for use in Equation 1. For the low-*Ri* case when the lutocline layer is turbulent, F_s may vary vertically.

Settling rates of cohesive sediments vary widely. Fluid mud settling is normally in the hindered range; that is, settling rate decreases with increased suspension concentration. Over most of the concentration range, cohesive suspensions settle as a mass. Settling rate is, therefore, a property of the overall suspension rather than of the individual particles it contains. Larger silt particles and clay aggregates or flocs all settle together because interparticle interactions prevent separation and sorting by grain characteristics.

Wolanski and others (1992) showed that fluid mud settling decreases drastically if the fluid mud layer is mixed. Decreases were observed in settling at the interface by factors of 3 to 10 in the presence of small amounts of turbulence. Mixing or shearing disrupts microchannel fluid pathways important to the upward flow accompanying hindered settling.

Within the fluid mud concentration range, at least one concentration value can be found at which settling flux is a local maximum. This occurs typically at 5 g/L or greater concentration depending on the sediment. Where these concentrations occur, interfaces form with abrupt vertical concentration and density change where internal waves can form. While it is not known exactly what role these discontinuities play, it seems likely they influence the vertical structure of lutoclines and, thus, entrainment. Settling flux maxima are also sediment dependent.

The effects of settling on entrainment have been detected experimentally and reported by Wolanski (1972). Salt- and kaolinite-stratified entrainment data from oscillating-grid experiments are shown in Figure 6a. These tests

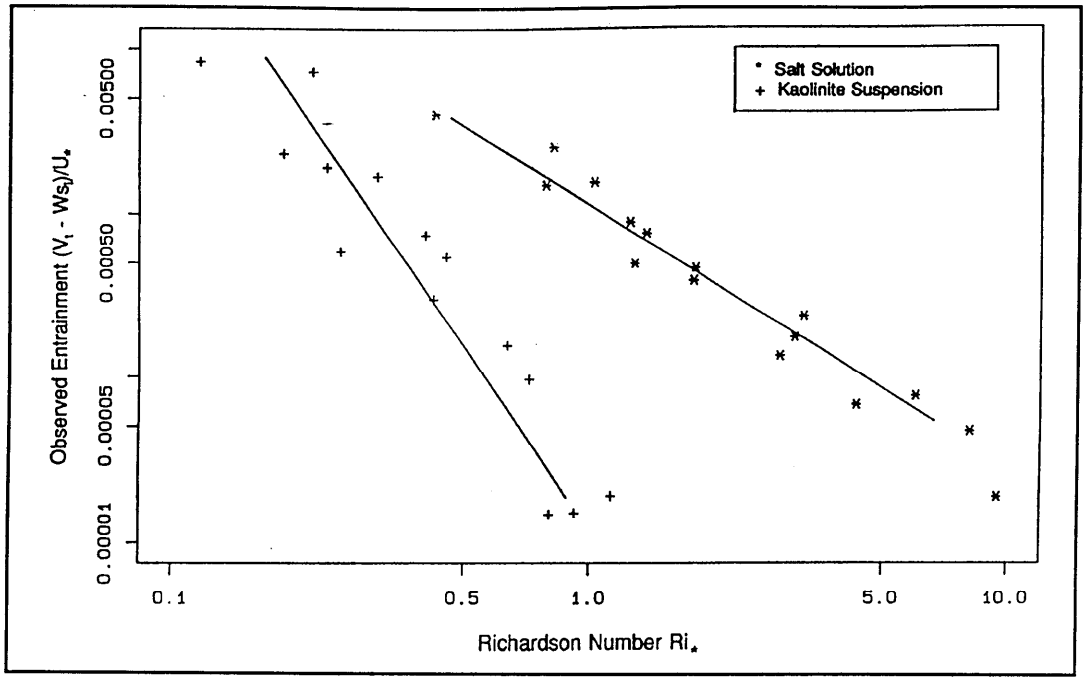

(a)

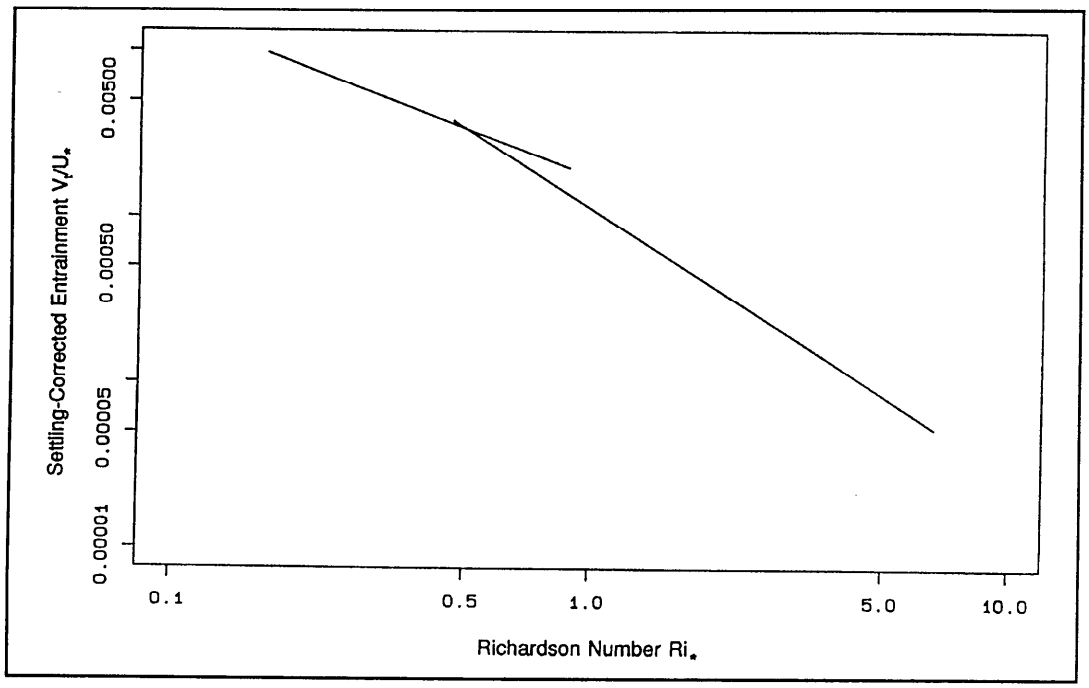

(b)

Figure 6. Original observed dense fluid and fluid mud entrainment rates (a) from Wolanski (1972) and (b) turbulent entrainment components estimated by adding a constant settling term

used a chamber where turbulence was generated by an oscillating grid rather than by a shear flow, such as would be the case in a flume or open channel. For these tests, the Richardson number, Ri_*, is defined based on shear velocity, U_*, instead of U, and $U_* = \omega a$, where ω is the angular rate of oscillation and a is the amplitude. The clay suspensions had low viscosity, and suspension concentrations were on the order of 3 g/L. As noted earlier, kaolinite has settling rates about an order of magnitude lower than many natural cohesive sediments.

The observed entrainment for the kaolinite suspension shown in Figure 6a included the effects of settling and was much lower than for the salt solution. Furthermore, it was reported that E approached zero at $Ri_* = 2$ as a result of settling, so that settling flux was on the same order as turbulent entrainment flux, F_t, at this point. The lines in Figure 6a associated with the data points are the original author's fit to the data. The data show that a power law is a reasonable approximation to the relationship between E and Ri_*. There is an appreciable difference between $(V_t - Ws_i)/U_*$ versus Ri_* relationships for salt and for kaolinite suspensions obtained in the same experimental apparatus which can be explained by settling effects.

The effect of settling can be demonstrated by adding an estimate of Ws_i/U_* to the original observed entrainment $(V_t - Ws_i)/U_*$. Tests on kaolinite suspensions were performed at concentrations of only about 3 g/L. Under these conditions the density or concentration jump across the lutocline is small, and Ws_i approaches Ws. Settling rate was not measured. However, a Ws value of 0.1 mm/sec is representative of the maximum settling rate for kaolinite (which was likely to have occurred at this low concentration) and was assumed. Figure 6b shows a plot of how the salt and kaolinite suspension data lines adjusted to yield V_t/U_*. Since for salt $Ws = 0$, the V_t/U_* line for the salt solution is identical to the line in Figure 6a. The assumed constant settling rate brought the V_t/U_* line for the kaolinite suspension in fair agreement with the salt tests, indicating that the turbulent entrainment, F_t, was equivalent for both series of tests.

Stable- and Dense-Layer Thickness

Entrainment across a density interface causes a lutocline to form at the top of the dense layer, as previously described. The thickness of the salt-stratified stable layer, h, has been found to depend on the depth, D, of the mixed layer, and

$$h = 0.06\,D \tag{11}$$

Under these conditions, the lutocline resembles the low-current case shown in Figure 1. This relationship was confirmed for the moderate-Ri_u kaolinite entrainment shown in Figure 2 (Srinivas and Mehta 1989). However, at lower Ri values, Wolanski and others (1988, 1992) showed that the

lutocline layer thickness during fluid mud entrainment is a balance between the shear velocity, settling rate, and overall density difference across the lutocline, and that

$$h = \frac{4\,U_*^3}{Ws\,\Delta b} \tag{12}$$

describes the thickness of the lutocline layer. Under these conditions, the lutocline layer resembles the high-current case shown in Figure 1. The Δb here refers to the difference between the lutocline layer and the mixed layer. Field observations show that the lutocline layer can occupy more than half the water column depth, D. Lutoclines 1 to 5 m thick have been observed where currents were on the order of 1 m/sec.

Many dredged material layers are initially of limited thickness after disposal. For instance, the fluid mud underflow at a Tylers Beach, Virginia, pipeline discharge was predicted to be only about 0.03 D (Appendix A; Thevenot, Prickett, and Kraus 1992). Fluid mud thicknesses are often too small to be reliably observed in the field.

When the dense layer is thin relative to the mixed layer, say <0.06 D, vertical velocity fluctuations may be suppressed by the rigid layer below the dense layer. Penetration of the dense layer by turbulent motions might also be suppressed. A set of tests were carried out to test this hypothesis since no information on this effect was found in the literature.

To test the effects of thin dense-layer thickness on entrainment rates, a series of tests were performed using the newly developed particle erosion simulator (PES) device. The DRP adopted this device to characterize cohesive sediment erodibility. The heart of the PES is a cylindrical chamber (5 in. (12 cm) in diameter; 5 in. high) that contains an oscillating grid. This general type of device has been used extensively in entrainment experiments, although the PES has additional features to handle fine-grained sediments. The PES will be described in more detail in a future Dredging Research Technical Note. The PES was used to test salt brine dense layers (density of about 1.19 g/cu cm) that had limited thicknesses. Tap water was used as the mixed-layer fluid.

At the beginning of the tests, the dense layer was injected under the mixed layer in the chamber and the water depth of the mixed layer adjusted to 5 in. The initial thickness of the dense layer was varied in ten tests from 1.5 to 0.4 in. (3.8 to 1 cm) or from 0.3 to 0.08 D. During individual tests, grid oscillation rates were increased in steps, dense layer thicknesses were observed using dye, and samples of the mixed layer were taken. From precise determination of salinity of the mixed layer, entrainment rates were calculated for each test step. The experimental

results were nondimensionalized by plotting entrainment per oscillation versus Ri_*.

Results shown in Figure 7 indicate that there was no discernible effect of dense layer thickness on entrainment rate. Based on these results, dredged material layers of limited thickness would be expected to entrain as described earlier.

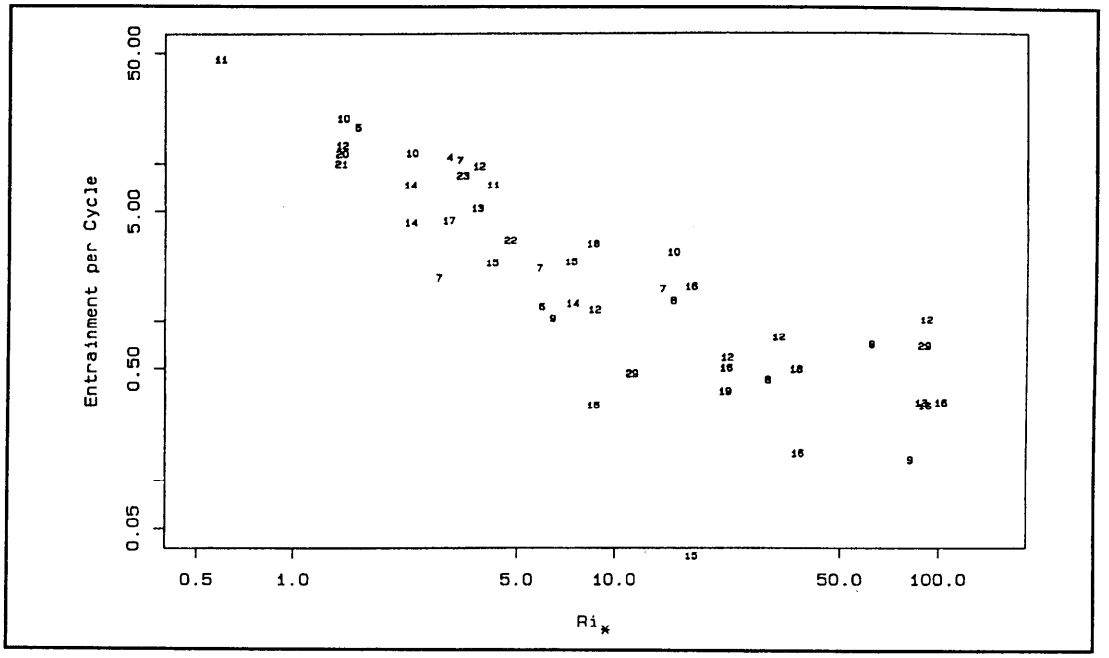

Figure 7. Entrainment for various dense layer thicknesses (numbers indicate thickness relative to D as a percent)

Application of Proposed Entrainment Algorithm

Density stratification, settling, and viscosity can be important entrainment mechanisms as shown earlier. Algorithms proposed for entrainment under various conditions can be used to make estimates of dispersion from the vicinity of a disposal site. Information on the density of the fluid mud layer, its settling and viscous properties, and ambient flow conditions at the site are required. Estimates of dredged material density following disposal could be made by a separate model for near-field dilution, such as the STFATE model described in *Dredging Research Technical Notes* DRP-1-04 (Johnson, Tallent, and Fong 1992) and DRP-1-10 (Nelson and Johnson 1992) or other models. Determination of sediment properties generally requires laboratory analysis.

Elaborations on steady-state solutions to Equations 3, 8, and 9 are necessary. For the steady-state assumption (where h and E are constant in

time) to be valid, entrainment, E , must be constant vertically across the lutocline. Equation 3 was developed for data for which F_t and E were constant in the vertical. Since concentration and F_s will vary vertically across the lutocline, F_t must also vary for E to be constant. (Also F_t must have a minimum value that is greater than the greatest F_s in the lutocline.) In the usual case where the dense layer concentration exceeds that at which maximum settling flux occurs, lutocline settling flux can be estimated as the maximum settling flux for that particular material. Use the maximum settling flux to compare to a calculated F_t. If the settling flux, F_s , is even as large as 0.25 F_t , entrainment might increase with depth in the lutocline and the steady-state assumption may not be valid.

Lutocline thickness, h, should be estimated using Equation 12. If the result is much greater than 0.06 D, Equations 3, 8, and 9 should be used with caution. Numerical solution methods for Equations 4 and 5 might be required.

When the greatest level of accuracy is needed or other circumstances dictate, the proposed algorithm can be used as part of a numerical solution scheme that includes feedbacks between conditions of the mixed, stable, and dense layers. Such procedures are being incorporated into a DRP personal computer program now under development.

Though only one application has been made thus far, results appeared to overpredict entrainment somewhat (Thevenot, Prickett, and Kraus 1992). The proposed entrainment algorithms will continue to be tested against existing field information and any new monitoring data on dense layer behavior in the field that becomes available.

For the case of negatively buoyant plumes from continuous or instantaneous dredged material discharges, entrainment is not inhibited by density differences, although cohesive sediment viscosity may inhibit entrainment. Descriptors of viscous mechanisms that might suppress entrainment could be incorporated into numerical model formulations.

References

Bowers, G. W., and Goldenblatt, M. K. 1978. "Calibration of a Predictive Model for Instantaneously Discharged Dredged Material," EPA-600/3-78-089, Corvallis Environmental Research Laboratory, U.S. Environmental Protection Agency, Corvallis, OR.

Campbell, I. H., and Turner, J. S. 1986. "The Influence of Viscosity on Fountains in Magma Chambers," *Journal of Petrology*, Vol 27, Part 1, pp 1-30.

Johnson, B. H., Tallent, J. R., and Fong, M. T. 1992. "Numerical Disposal Modeling Needs Revealed by Mobile Bay Field Data," *Dredging Research Technical Notes* DRP-1-04, U.S. Army Engineer Waterways Experiment Station, Vicksburg, MS.

Narimousa, S., and Fernando, H. J. S. 1987. "On the Sheared Density Interface of an Entraining Stratified Fluid," *Journal of Fluid Mechanics*, Vol 174, pp 1-22.

Nelson, E. E., and Johnson, B. H. 1992. "Analysis of Dredging Material Deposition Patterns," *Dredging Research Technical Notes* DRP-1-10, U.S. Army Engineer Waterways Experiment Station, Vicksburg, MS.

Srinivas, R., and Mehta, A. J. 1989. "Observations on Estuarine Fluid Mud Entrainment," *International Journal of Sediment Research*, Vol 5, No. 1, pp 15-22.

Teeter, A. M. 1992a. "Erosion of Cohesive Dredged Material in Open-Water Disposal Sites," *Dredging Research Technical Notes* DRP-1-07, U.S. Army Engineer Waterways Experiment Station, Vicksburg, MS.

_____. 1992b. "The Viscous Characteristics of Channel-Bottom Muds," *Dredging Research Technical Notes* DRP-2-04, U.S. Army Engineer Waterways Experiment Station, Vicksburg, MS.

_____. 1994. "Water Wave Attenuation over Nearshore Underwater Mudbanks and Mud Berms," *Dredging Research Technical Notes* DRP-1-14, U.S. Army Engineer Waterways Experiment Station, Vicksburg, MS.

Teeter, A. M., and Pankow, W. 1989. "Schematic Numerical Modeling of Harbor Deepening Effects on Sedimentation, Charleston, South Carolina," Miscellaneous Paper HL-89-7, U.S. Army Engineer Waterways Experiment Station, Vicksburg, MS.

Thevenot, M. M., Prickett, T. L., and Kraus, N. C., eds. 1992. "Tylers Beach, Virginia, Dredged Material Plume Monitoring Project, 27 September to 4 October 1991," Technical Report DRP-92-7, U.S. Army Engineer Waterways Experiment Station, Vicksburg, MS.

Wolanski, E. J. 1972. "Turbulent Entrainment Across Stable Density-Stratified Liquids and Suspensions," Ph.D. dissertation, Johns Hopkins University, Baltimore, MD.

Wolanski, E. J., Chappell, J., Ridd, P., and Vertessy, R. 1988. "Fluidization of Mud in Estuaries," *Journal of Geophysical Research*, Vol 93, No. C3, pp 2351-2361.

Wolanski, E. J., and others. 1992. "The Role of Turbulence in the Settling of Mud Flocs," *Journal of Coastal Research*, Vol 8, No. 1, pp 35-46.